Progress In Electromagnetics Research, PIER 81, 73–97, 2008

TRUNCATED COSINE FOURIER SERIES EXPANSION METHOD FOR SOLVING 2-D INVERSE SCATTERING PROBLEMS

A. Semnani and M. Kamyab

Department of Electrical Engineering
K. N. Toosi University of Technology
P.O. Box 16315-1355, Tehran, Iran

Abstract—Truncated cosine Fourier series expansion method is applied for reconstruction of lossy and inhomogeneous 2-D media by using inverse scattering method in time domain. In this method, the unknown parameters are expanded in a cosine Fourier series and coefficients of this expansion are optimized in particle swarm optimization (PSO) routine with the aid of finite difference time domain (FDTD) method as an electromagnetic (EM) solver. The performance of the algorithm is studied for several 2-D permittivity and conductivity profile reconstruction cases. It is shown that since only a limited number of terms are retained in the expansion, using the proposed method guarantees the well-posedness of the problem and uniqueness of the solution and various types of regularization may be used to only have more precise reconstruction. It is also shown that the number of unknowns in optimization routine is reduced more than 75 percent as compared with conventional methods which leads to a considerable reduction in the amount of computations with negligible adverse effect on the precision of reconstruction. Sensitivity analysis of the suggested method to the number of expansion terms in the algorithm is studied, as well.

1. INTRODUCTION

In an inverse scattering problem, one tries to reconstruct or identify an object based on data available through EM field components back scattered from object illuminated by known incident wave. The data needed for such purpose may be collected for example from measurements or design objective.

Inverse scattering has gained considerable attention because of its vast applications in different branches of science such as medical tomography, non-destructive testing, object detection, geophysics, ground penetrating radars, remote sensing, atmospheric science and optics [1–7].

Three important issues must be preliminary considered in an inverse scattering problem; the non-uniqueness, the ill-posedness, and the intrinsic nonlinearity [8–10]. The first two items appear because the operator that maps the scatterer properties to the scattered field is compact. The non-uniqueness and the ill-posedness can be treated by using regularization schemes [11–17]. On the other hand, the nonlinearity emerges from the fact that the scattered field is a nonlinear function of the electromagnetic properties of the scatterers due to multiple scattering phenomena. The nonlinearity of the problem is handled by applying iterative optimization techniques.

Recently, inverse scattering problems are studied in global optimization-based procedures. The unknown parameters of each cell of the medium grid would be directly considered as the optimization parameters. Therefore, the general form of cost function for optimization routine can be expressed as

$$F\left(\varepsilon_r,\,\sigma,\,\mu,\,\vec{E},\,\vec{H}\right) = \sum_{i=1}^{I}\sum_{j=1}^{J}\int_0^T \left(\left\|\vec{E}_{ij}^{sim}-\vec{E}_{ij}^{meas}\right\|^2+\eta_0^2\left\|\vec{H}_{ij}^{sim}-\vec{H}_{ij}^{meas}\right\|^2\right)dt \tag{1}$$

where $\vec{E}^{sim}$ and $\vec{H}^{sim}$ are the simulated fields obtained by the FDTD method [18] in each optimization iteration. $\vec{E}^{meas}$ and $\vec{H}^{meas}$ are measured fields, I and J are the number of transmitters and receivers, respectively and T is the total time of measurement. On the other hand, as discussed before, regularization must be used to overcome the intrinsic ill-posedness and non-uniqueness of the inverse problem. Hence, the cost function should be modified as

$$F\left(\varepsilon_r,\,\sigma,\,\mu,\,\vec{E},\,\vec{H}\right) = \sum_{i=1}^{I}\sum_{j=1}^{J}\int_0^T \left(\left\|\vec{E}_{ij}^{sim}-\vec{E}_{ij}^{meas}\right\|^2+\eta_0^2\left\|\vec{H}_{ij}^{sim}-\vec{H}_{ij}^{meas}\right\|^2\right)dt + \lambda\times R\left(\varepsilon_r,\,\sigma,\,\mu\right) \tag{2}$$

Here $R(\varepsilon_r,\,\sigma,\,\mu)$ is the regularization term and λ is the regularization factor.

Unfortunately, the conventional optimization-based methods stated above suffer from two main drawbacks. The first is the huge

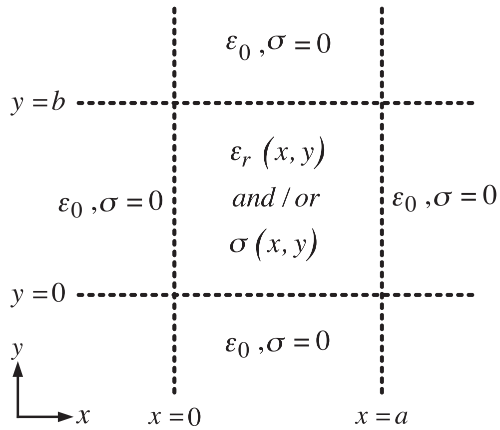

Figure 1. General form of the problem. Reconstruction of the permittivity and conductivity profiles of a lossy and inhomogeneous 2-D medium surrounded by known media (here free space) is considered.

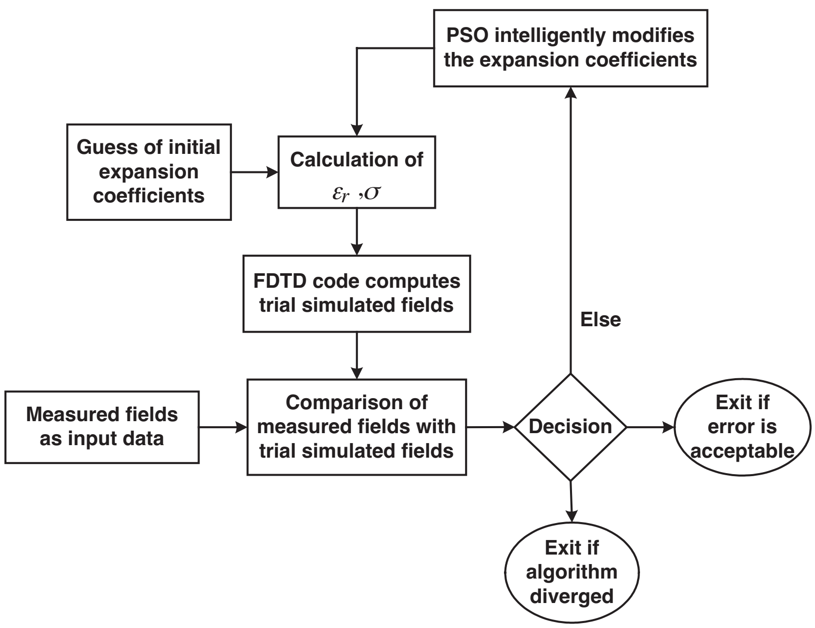

Figure 2. Block diagram of the expansion method for solving inverse scattering problems [19].

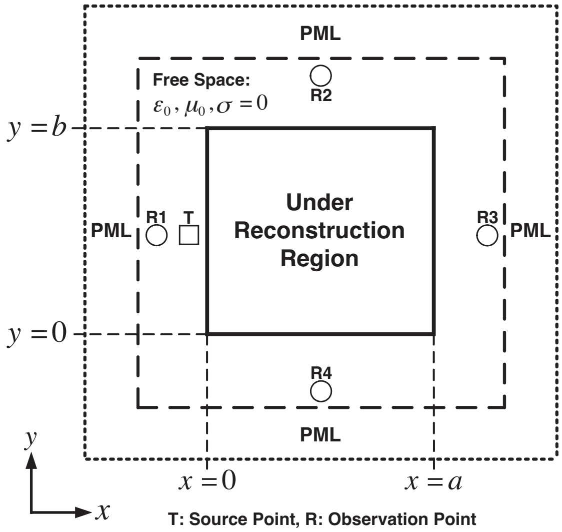

Figure 3. Geometrical configuration of the problem. One transmitter and four receivers are used in all case studies.

number of the unknowns especially in two-dimensional (2-D) and three-dimensional (3-D) cases which increases not only the amount of computations, but also the degree of ill-posedness. Another disadvantage is the determination of regularization factor which is rather a difficult task. Therefore, the truncated cosine Fourier series expansion method which reduces the amount of computations along with the sensitivity of the algorithm to the regularization term has been introduced [19]. With the help of this algorithm, it is possible to use (1) instead of (2) with assurance about the well-posedness of the problem.

In this paper, the truncated cosine Fourier series expansion method is applied for computationally efficient reconstruction of 2-D inhomogeneous and lossy structures. The general form of the problem, the expansion method and the mathematical considerations of the method are explained in Section 2. In Section 3, several 2-D inhomogeneous and lossless or lossy case studies are considered and the efficiency of the method is studied for all of them. Finally in Section 4, two important issues regarding sensitivity considerations of the proposed expansion method are addressed.

2. TRUNCATED COSINE FOURIER SERIES EXPANSION METHOD FOR 2-D PROBLEMS

Use of 2-D approximation simplifies the computations since the problem is generally reduced from vectorial to scalar which decreases the dimension of the solution space significantly. Despite the approximation, the 2-D assumption is appropriate in many cases and there are good examples of good 2-D imaging algorithms which have proven to be quite useful in practice [1, 5, 6, 15].

The permittivity and conductivity profiles reconstruction of a lossy and inhomogeneous 2-D region as shown in Fig. 1 is considered.

It has been shown [19–21] that instead of direct optimization of the unknowns, we can expand them in terms of a complete set of orthogonal basis functions and optimize the coefficients of the expansion in a global optimization routine like PSO [22–24]. If cosine basis functions are used for our 2-D case, the expansion of the relative permittivity profile in transverse x-y plane which is homogeneous along z can be written as

$$\varepsilon_r(x, y) = \sum_{n=0}^{N} \sum_{m=0}^{M} d_{nm} \cos\left(\frac{n\pi}{a}x\right) \cos\left(\frac{m\pi}{b}y\right) \tag{3}$$

where a and b are the dimensions of the problem in the x and y directions, respectively and the coefficients, d_{nm}, are to be optimized. In this case, the number of optimization parameters is $(N+1) \times (M+1)$ in comparison with conventional methods in which this number is equal to the number of grid points. This results in a considerable reduction in the amount of computations. The block diagram of the applied algorithm is illustrated in Fig. 2.

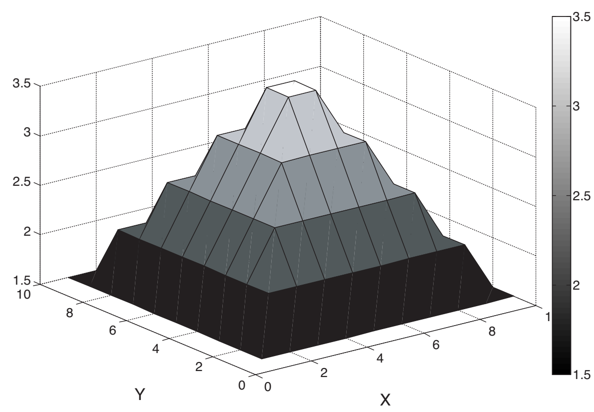

(a)

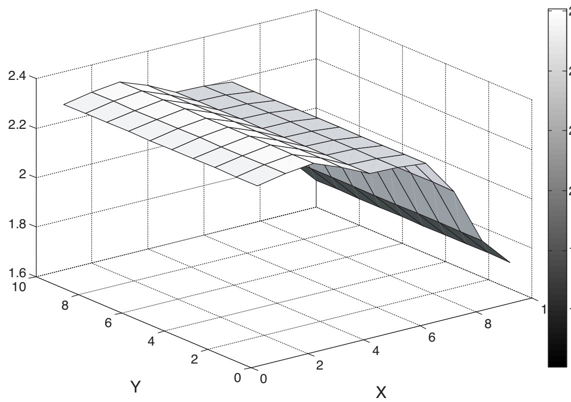
2.4
2.2
2
1.8
1.6
10
8
6
4
2
0
Y
0
2
4
6
8
X
2.3
2.2
2.1
2
1.9
1.8

(b)

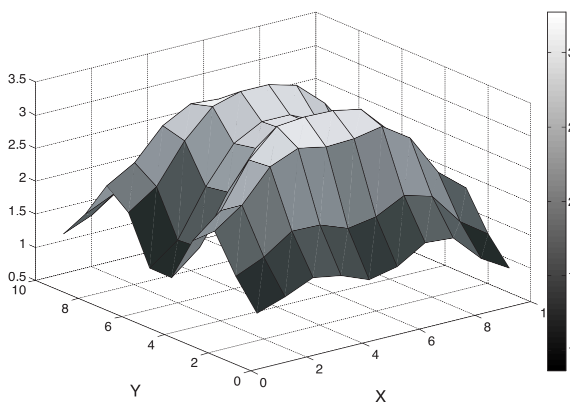
3.5
3
2.5
2
1.5
1
0.5
10
8
6
4
2
0
Y
0
2
4
6
8
X
3
2.5
2
1.5
1

(c)

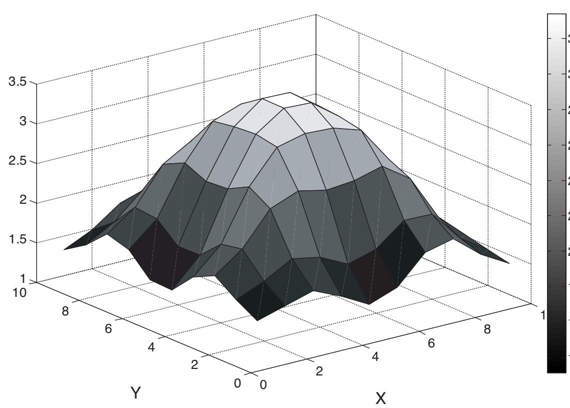
3.5
3
2.5
2
1.5
1
10
8
6
4
2
0
Y
0
2
4
6
8
X
3.2
3
2.8
2.6
2.4
2.2
2
1.8
1.6
1.4

(d)

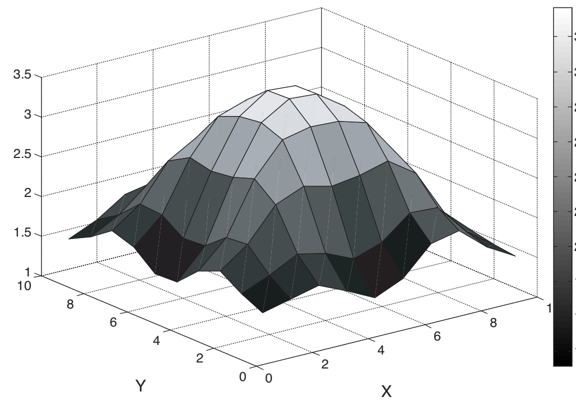

(e)

Figure 4. Permittivity profile reconstruction of case study #1 by using the expansion method without regularization. (a) Original profile, (b) Initial guess, (c) Reconstruction after 30 iterations, (d) Reconstruction after 100 iterations, and (e) Reconstruction after 200 iterations.

According to Fig. 2, based on an initial guess for a set of expansion coefficients, d_{nm}, for a lossless case for instance, the relative permittivity is calculated based on (3). Then, FDTD code computes trial electric and magnetic simulation fields. Here we use a Gaussian

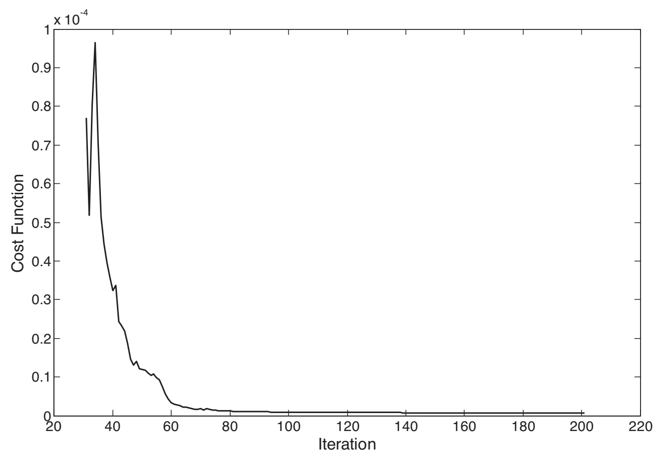

Figure 5. Cost function of optimization routine for permittivity profile reconstruction of case study #1.

pulse for excitation and UPML [18] for truncation of the problem space in FDTD simulations. In our study, due to the lack of real measurement data, measured fields are also obtained by an FDTD direct simulation. In each step of optimization routine, the cost function is calculated. Then PSO as a global optimizer is used to minimize this cost function by changing the coefficients of relative permittivity and conductivity profiles expansions, iteratively.

Since inverse problems are non-unique and ill-posed in nature, a priori information must be applied for stabilizing the algorithm as much as possible. To achieve this, we may impose two physical constraints on the unknown parameters of the medium. First, it is

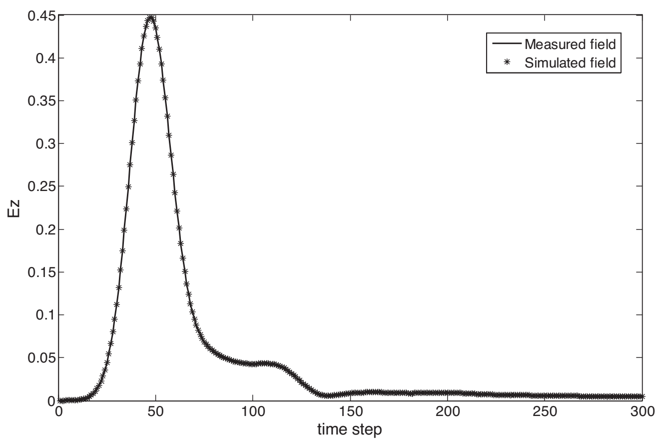

(a)

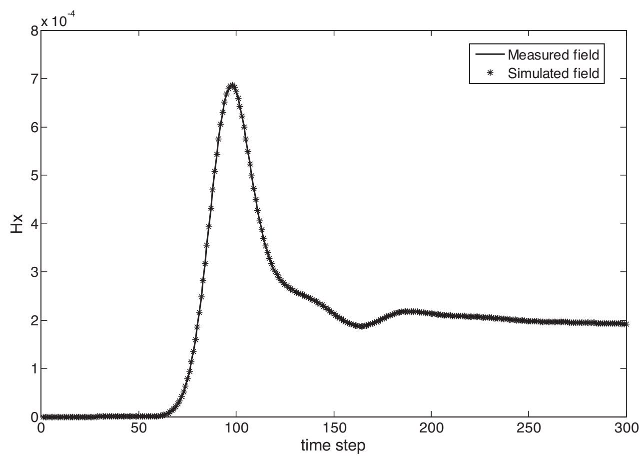

(b)

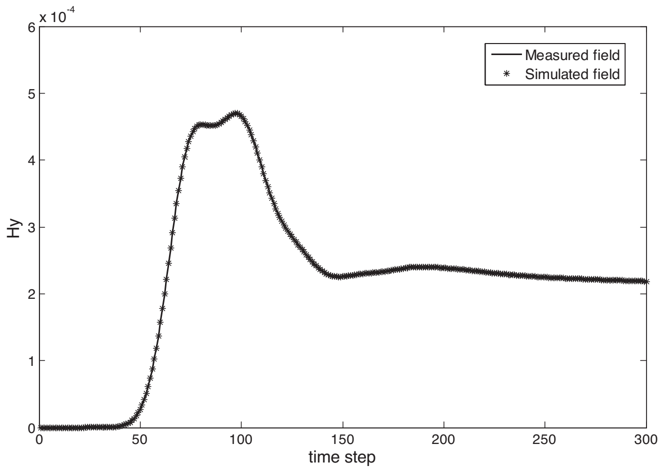

(c)

Figure 6. Comparison of measured and simulated fields in reconstruction of case study #1. (a) E_z field in observation point #1, (b) H_x field in observation point #3, (c) H_y field in observation point #4.

assumed that the relative permittivity and conductivity have limited ranges of variation which is reasonable for real structures, i.e.,

$$1 \leq \varepsilon_r\,(x,\,y) \leq \varepsilon_{r,\,\max} \tag{4}$$

and

$$0 \leq \sigma\,(x,\,y) \leq \sigma_{\max} \tag{5}$$

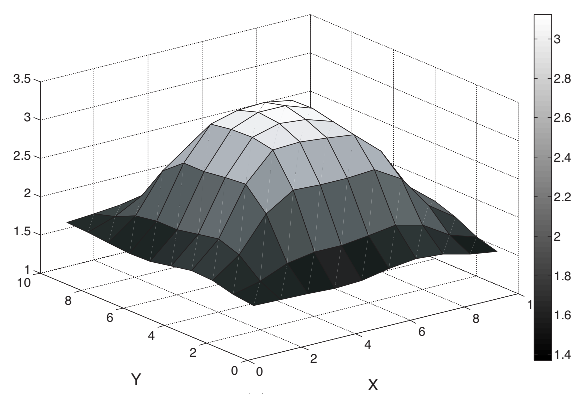

(a)

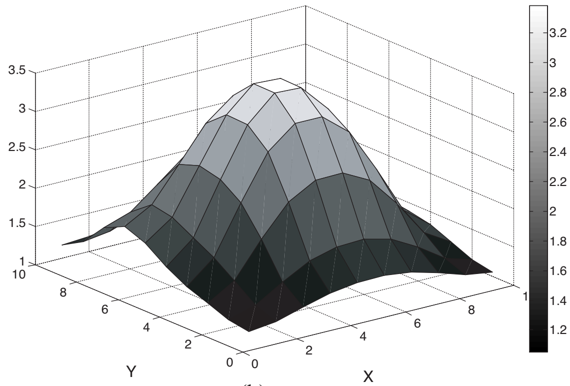

(b)

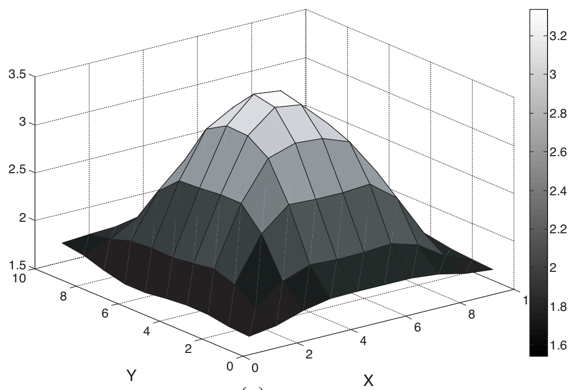

(c)

Figure 7. Permittivity profile reconstruction of case study #1 by using (a) Tikhonov energy regularization, (b) second order Sobolev regularization, and (c) TV regularization.

The second assumption is that the permittivity and conductivity profiles may not have severe fluctuations or oscillatory behaviour. According to what follows, these two important conditions are reflected on expansion coefficients as physical constraints during the optimization process.

It is known that average of a function with known limited range is located within that limit, that is if

$$L_1 \leq f(x,\, y) \leq L_2, \quad \begin{cases} x_1 \leq x \leq x_2 \\ y_1 \leq y \leq y_2 \end{cases} \tag{6}$$

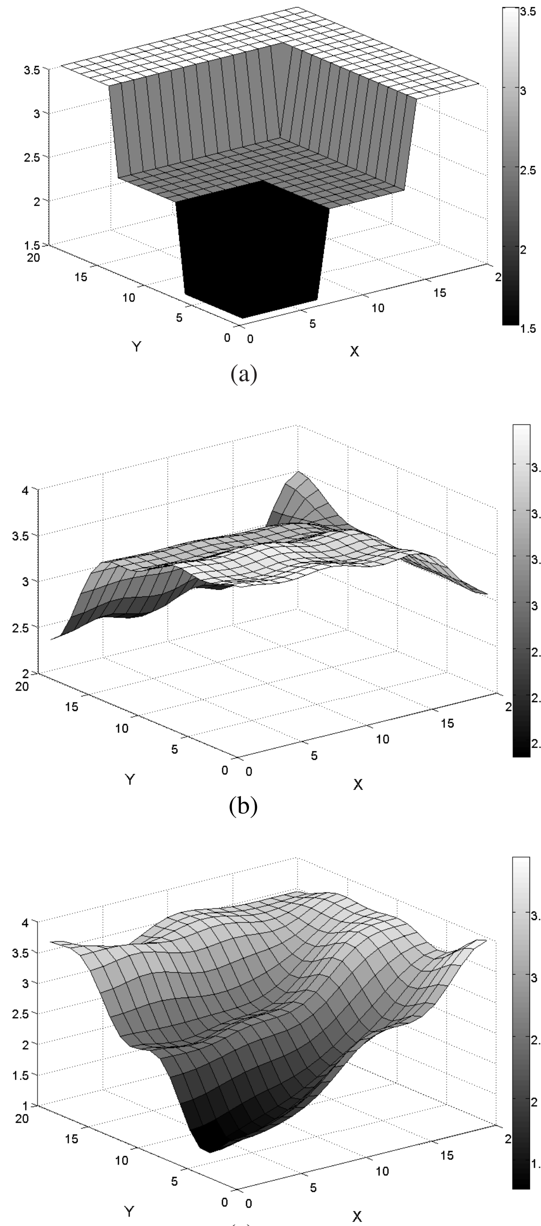

(a)

(b)

(c)

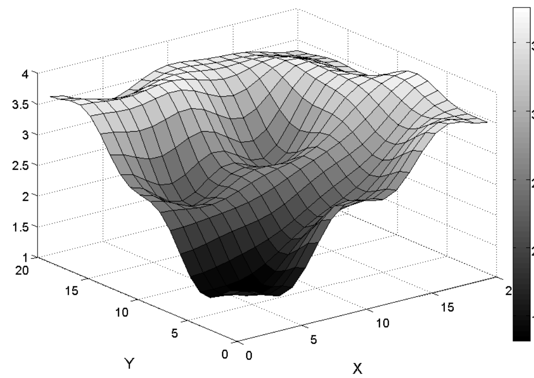

(d)

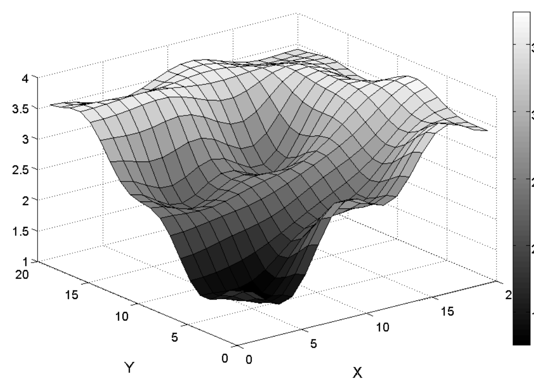

(e)

Figure 8. Permittivity profile reconstruction of case study #2 by using the expansion method without regularization. (a) Original profile, (b) Initial guess, (c) Reconstruction after 30 iterations, (d) Reconstruction after 100 iterations, and (e) Reconstruction after 200 iterations.

Then

$$L_1 \leq \frac{1}{(x_2 - x_1)(y_2 - y_1)} \int_{x_1}^{x_2} \int_{y_1}^{y_2} f(x, y)\, dy dx \leq L_2 \tag{7}$$

Thus, for relative permittivity profile expansion we have

$$1 \leq d_{00} \leq \varepsilon_{r,\max} \tag{8}$$

For $x = 0$ and $y = 0$, (3) reduces to

$$\varepsilon_r(0,\,0) = \sum_{n=0}^{N}\sum_{m=0}^{M} d_{nm} \quad \Rightarrow \quad 1 \leq \sum_{n=0}^{N}\sum_{m=0}^{M} d_{nm} \leq \varepsilon_{r,\,\max} \tag{9}$$

and for $x = a$ and $y = b$, we have

$$\varepsilon_r(a,\,b) = \sum_{n=0}^{N}\sum_{m=0}^{M} (-1)^{n+m}\, d_{nm} \;\Rightarrow$$
$$1 \leq \sum_{n=0}^{N}\sum_{m=0}^{M} (-1)^{n+m}\, d_{nm} \leq \varepsilon_{r,\,\max} \tag{10}$$

Using Parseval theorem, another relation between expansion coefficients and upper bound of relative permittivity may be written. That is

$$\frac{1}{(x_2 - x_1)(y_2 - y_1)} \int_{x_1}^{x_2} \int_{y_1}^{y_2} |f\,(x, y)|^2 \, dydx = \sum_{n=0}^{N}\sum_{m=0}^{M} |d_{nm}|^2 \tag{11}$$

Based on (3), (11) may be simplified as

$$1 \leq \sum_{n=0}^{N}\sum_{m=0}^{M} |d_{nm}|^2 \leq \varepsilon_{r,\,\max}^2 \tag{12}$$

By using (8), (9), (10) and (12) in the initial guess of the expansion coefficients and as the damping boundary condition [22] during the optimization process, the routine converges in a considerable faster rate. Similar conditions can be used for conductivity profiles in lossy cases.

3. SIMULATION RESULTS

The proposed expansion method is utilized for three different cases. In the simulations of all case studies, one transmitter ($I = 1$) and four receivers ($J = 4$) are used around the under reconstruction medium as shown in Fig. 3. The population in PSO algorithm is chosen equal to 50, the maximum iteration is considered to be 200 and the number of time steps is limited to $T = 300$. A Gaussian waveform is used in the source point as the excitation.

Case study #1: In the first sample case, we consider an inhomogeneous and lossless 2-D medium consisting 10×10 cells.

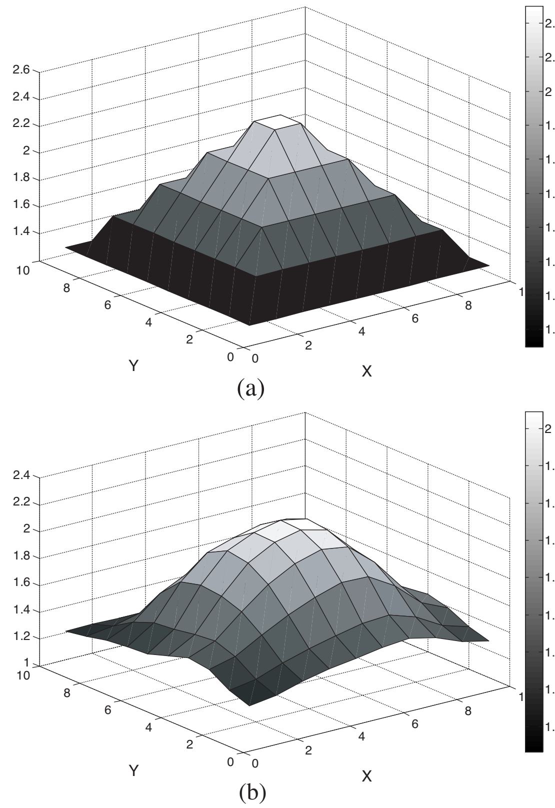

Figure 9. Permittivity profile reconstruction of case study #3 by using expansion method with the help of second order Sobolev regularization. (a) Original profile and (b) Reconstructed profile.

Therefore, only the permittivity profile reconstruction is considered. In the expansion method, the number of expansion terms in both x and y directions are set to 5 ($N = M = 4$). Thus, instead of 100 unknowns in direct optimization method we only have 25 unknowns in expansion method. This means 75 percent reduction in the number of unknowns which results in decreasing the required number of particles and iterations in the optimization routine.

The reconstructed profiles with the use of expansion method in several optimization iterations are shown in Fig. 4. As can be seen, a completely random initial expansion coefficients lead to a really drastic permittivity profile as starting point in iteration process according to Fig. 4(b). However, the algorithm which uses a global optimization

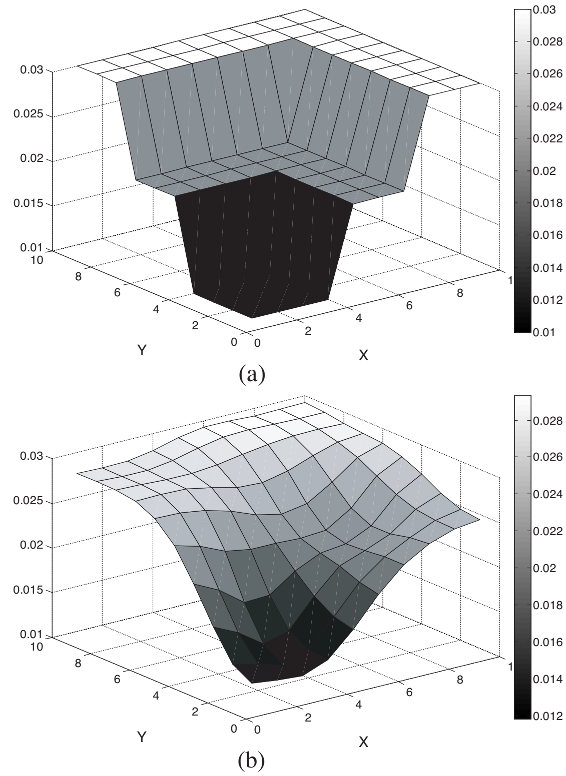

Figure 10. Conductivity profile reconstruction of case study #3 by using expansion method with the help of second order Sobolev regularization. (a) Original profile and (b) Reconstructed profile.

routine has the ability of good reconstruction according to Fig. 4(e). Also, inspection of the results indicates that the algorithm has a relatively fast convergence rate.

The cost function (1) is graphed versus the iteration number in Fig. 5. It is seen that the PSO as a powerful global optimization method reduces the cost function quickly in this 5×5 2-D case. It is to be noted that due to drastic variations of cost function at the beginning iterations which cause the unrealizable changes in remaining iterations, the cost function is plotted from 30th iteration.

According to (1), it is seen that least square criterion between measured and simulated electric and magnetic fields is used as cost function in this algorithm. As a check of method validity, the measured and simulated scattered fields of case study #1 in some different

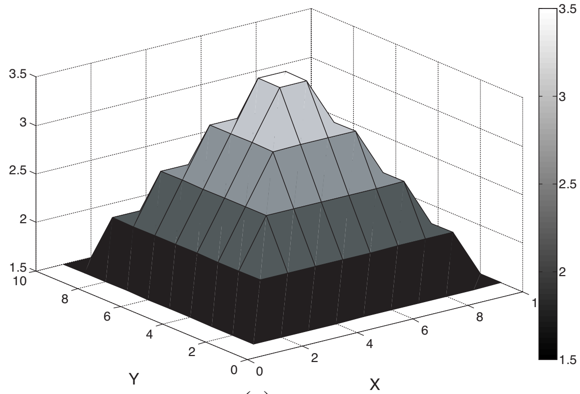
3.5
3
2.5
2
1.5
10
8
6
4
2
0
Y
0
2
4
6
8
X
3.5
3
2.5
2
1.5

(a)

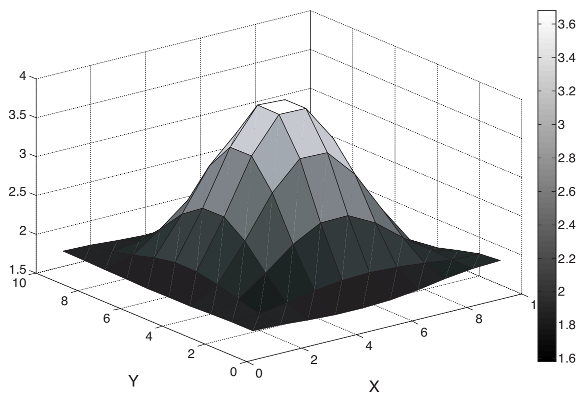
4
3.5
3
2.5
2
1.5
10
8
6
4
2
0
Y
0
2
4
6
8
X
3.6
3.4
3.2
3
2.8
2.6
2.4
2.2
2
1.8
1.6

(b)

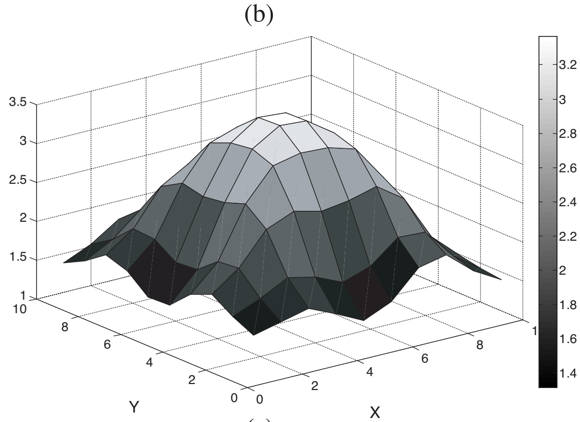
3.5
3
2.5
2
1.5
1
10
8
6
4
2
0
Y
0
2
4
6
8
X
3.2
3
2.8
2.6
2.4
2.2
2
1.8
1.6
1.4

(c)

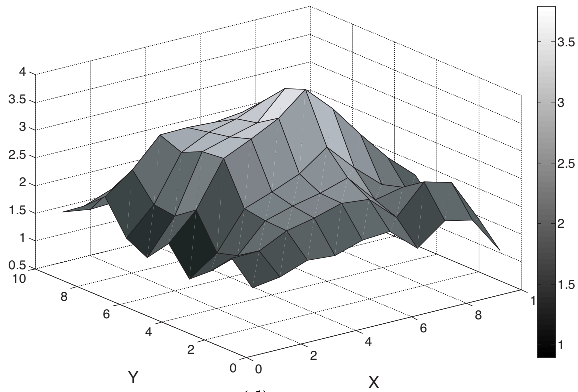

(d)

Figure 11. Comparison of reconstructions by the expansion method with different number of expansion terms for case study #1. (a) Original profile, (b) $N = M = 3$, (c) $N = M = 5$ and (d) $N = M = 8$.

observation points at the end of reconstruction process for this TM_z case are plotted in Fig. 6. It can be seen that the simulated fields are completely coincide with measured ones.

As mentioned before, various kinds of regularization terms may be used to have more precise reconstruction. To investigate this, we have used the expansion method with the help of Tikhonov energy regularization [11], second order Sobolev regularization [12] and total variation (TV) regularization [13] with $N = M = 4$ according to (2) for reconstruction of case study #1. The results are shown in Fig. 7. Although some improvement are observed especially by using second order Sobolev and TV regularizations, but the differences is not very significant. Also, the optimized Fourier series expansion coefficients for reconstruction of case study #1 without and with regularization terms are depicted in Table 1 for comparison. It is seen that the coefficients of expansion are close to each other especially in lower frequencies.

It should be noted from the above reconstruction results that in spite of a valuable reduction in the amount of computations in the proposed expansion method, the reconstructed profiles have quite acceptable precisions.

Case study #2: In the second example, another lossless and inhomogeneous medium with 20×20 cells is considered. In the expansion method, N and M are chosen equal to 5. Therefore the number of unknowns is reduced to about one-tenth. The reconstructed profiles by using the expansion method in different iterations of optimization routine are depicted in Fig. 8. The Fourier expansion

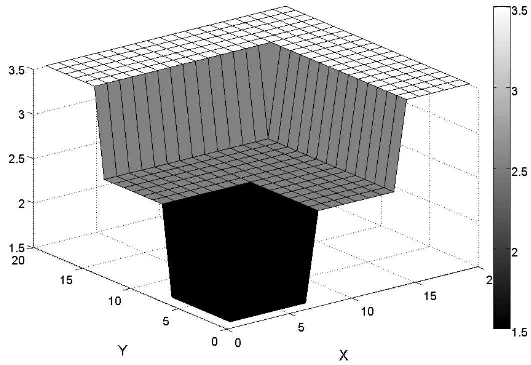
3.5
3
2.5
2
1.5
20
15
10
5
0
Y
0
5
10
15
2
X
3.5
3
2.5
2
1.5

(a)

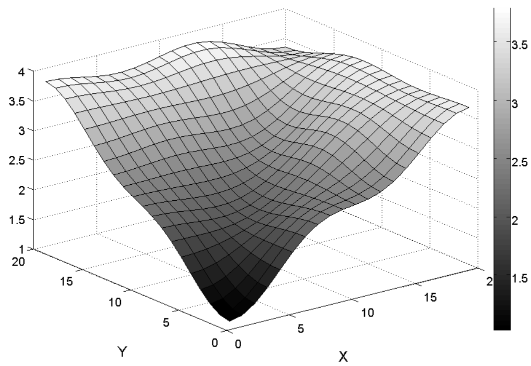
4
3.5
3
2.5
2
1.5
1
20
15
10
5
0
Y
0
5
10
15
2
X
3.5
3
2.5
2
1.5

(b)

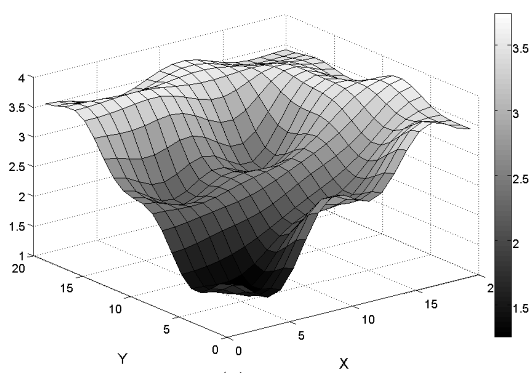
4
3.5
3
2.5
2
1.5
1
20
15
10
5
0
Y
0
5
10
15
2
X
3.5
3
2.5
2
1.5

(c)

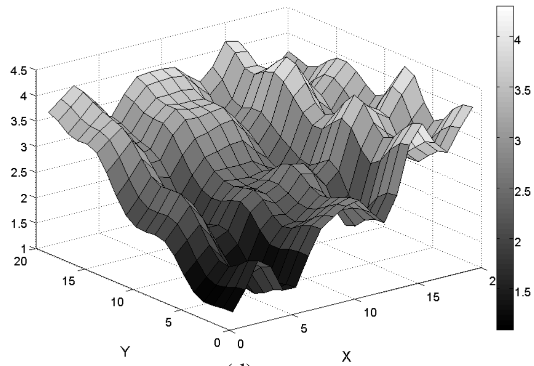

(d)

Figure 12. Comparison of reconstructions by the expansion method with different number of expansion terms for case study #2. (a) Original profile, (b) $N = M = 4$, (c) $N = M = 6$ and (d) $N = M = 10$.

coefficients for this case are represented in Table 2.

Case study #3: In this case, a lossy and inhomogeneous medium with 10×10 cells is considered. Therefore, we have two expansions for relative permittivity and conductivity profiles and in both expansions, N and M are chosen equal to 4. The reconstructed profiles of permittivity and conductivity by using second order Sobolev regularization are shown in Figs. 9 and 10, respectively. The Fourier expansion coefficients for this case for both profiles expansions are represented in Table 3.

The results for all three cases which are generally inhomogeneous and lossy or lossless media show that the proposed expansion method can tolerably reconstruct the unknown media with a considerable reduction in the amount of computations as compared to the conventional direct optimization of the unknowns.

4. SENSITIVITY CONSIDERATIONS

Regarding sensitivity of the algorithm, there are two important remarks we would like to explain. The first is that how the optimum number of expansion terms, N and M, should be chosen? Small values of N and M reduce the accuracy of reconstructed result, while large values cause oscillatory response or even divergence of the algorithm. This is clearly seen in the reconstructed profiles of Figs. 11 and 12 for case study #1 and #2, respectively. Our experiences from various permittivity and conductivity profiles reconstruction leads to

Table 1. Cosine Fourier series expansion coefficients (d_{nm}) for permittivity reconstruction of case study #1 (a) without regularization, (b) by using Tikhonov energy regularization, (c) by using second order Sobolev regularization, and (d) by using TV regularization.

n \ m	0	1	2	3	4
0	(a) 2.2271	0.0027	−0.4909	0.0036	−0.1743
	(b) 2.1758	−0.0171	−0.4435	−0.0137	−0.1392
	(c) 1.9827	0.0569	−0.6146	0.0228	−0.0499
	(d) 2.2181	−0.0112	−0.4925	−0.0152	−0.1095
1	−0.0004	−0.0047	0.0061	0.0716	−0.0277
	0.0076	−0.0152	0.002	0.0206	0.0065
	−0.0353	−0.0644	−0.0421	−0.0266	−0.0135
	−0.011	0.002	−0.0143	−0.0013	−0.0068
2	−0.4958	0.0163	0.4887	0.0394	−0.0163
	−0.5067	0.0391	0.3817	0.0219	0.0635
	−0.6409	−0.0293	0.4214	0.0062	0.0238
	−0.4275	−0.0195	0.4372	0.013	0.0289
3	0.0031	−0.0513	0.0268	0.0192	0.005
	0.0008	−0.0291	−0.0512	0.028	0.0023
	0.0239	0.0484	0.029	0.0173	0.0125
	−0.0021	−0.0028	−0.0492	0.0026	0.0082
4	−0.153	−0.0477	0.0153	−0.0125	0.0211
	−0.156	0.0067	0.0866	−0.0024	0.0471
	−0.1003	−0.0112	0.0514	−0.0123	0.0125
	−0.0959	0.0084	0.041	−0.0072	0.0563

the conclusion that choosing the number of expansion terms between 4 and 7 may be suitable for most of the 2-D reconstruction problems. The results shown in Figs. 11 and 12, confirm this idea for our two sample case studies.

The second important issue is that since the under reconstructed profiles are estimated by a truncated expansion in this algorithm, the number of required terms depends only on the profile variations

Table 2. Cosine Fourier series expansion coefficients (d_{nm}) for permittivity reconstruction of case study #2 without regularization.

n \ m	**0**	**1**	**2**	**3**	**4**	**5**
0	2.8772	−0.5342	0.1135	−0.0538	0.0041	0.0946
1	−0.5712	−0.5385	0.0027	−0.0593	0.0552	0.049
2	0.1102	0.0564	−0.1705	0.0205	0.0421	−0.0003
3	−0.0316	−0.0366	0.0292	−0.0275	−0.049	0.1276
4	0.0287	−0.0331	−0.0215	0.024	0.0281	0.0486
5	0.1727	0.0882	−0.032	−0.009	−0.0112	−0.0176

Table 3. Cosine Fourier series expansion coefficients (d_{nm}) for reconstruction of case study #3 by using second order Sobolev regularization. (a) permittivity and (b) conductivity expansion coefficients.

n \ m	**0**	**1**	**2**	**3**	**4**
0	(a) 1.5567 (b) 0.0236	−0.0293 −0.0025	−0.208 0.001	0.0279 0.0001	−0.0443 0.0004
1	0.0638 −0.0058	−0.0321 −0.0029	−0.0041 0.0005	0.008 0.0004	0.009 0.0005
2	−0.244 −0.0006	0.0236 −0.0016	0.1525 −0.001	−0.0062 0.0006	0.0259 −0.0001
3	0.0209 0.0003	−0.0066 0	−0.0302 −0.0001	0.001 0	−0.019 −0.0005
4	−0.0464 0	0.0059 0.0002	0.0141 0.0002	−0.0114 −0.0003	0.0067 −0.0002

and not on the dimensions of the region. Therefore, a brilliant advantage of this method is the possibility of reconstruction of large regions with only a few number of expansion terms. In Fig. 13, a permittivity profile similar to that of case study #1 but five times expanded is reconstructed tolerably by the expansion method with again $N = M = 4$. It means that a 2500 cell region is reconstructed with only 25 parameters which shows 99 percent reduction in the number of optimization parameters in comparison with conventional direct method.

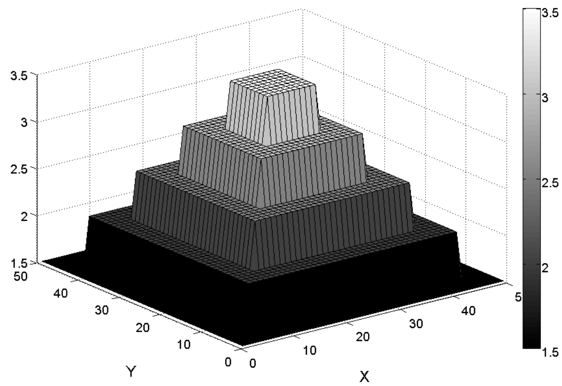

(a)

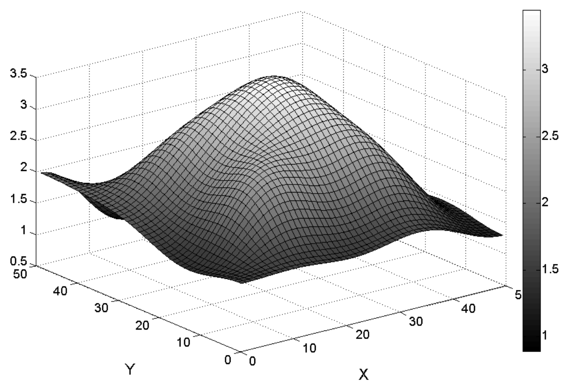

(b)

Figure 13. A 50×50 cell region permittivity profile reconstruction by the expansion method. (a) Original profile and (b) Reconstructed profile with $N = M = 4$.

5. CONCLUSION

A computationally efficient method which is based on combination of the cosine Fourier series expansion, the FDTD and the PSO algorithms has been applied for reconstruction of 2-D cases. The mathematical formulations of the method have been derived completely and the algorithm has been examined for reconstruction of several inhomogeneous lossless and lossy cases. With a considerable reduction in the number of the unknowns and consequently the required number of particles and optimization iterations as compared with conventional inverse scattering methods, the relative permittivity and conductivity profiles of 2-D media have been reconstructed successfully. It has been shown by sensitivity analysis that for obtaining well-posedness as well as accurate reconstruction simultaneously, the number of expansion terms must be chosen intelligently. Finally, it has been illustrated that due to the independence of the method on the region dimensions, it is possible to reduce the optimization parameters in the reconstruction of large regions, significantly.

ACKNOWLEDGMENT

This work was supported by the Iran Telecommunication Research Center (ITRC) under contract No. T-500-10528.

REFERENCES

1. Bindu, G., A. Lonappan, V. Thomas, C. K. Aanandan, and K. T. Mathew, "Active microwave imaging for breast cancer detection," *Progress In Electromagnetics Research*, PIER 58, 149–169, 2006.
2. Colton, D. and P. B. Monk, "Target identification of coated objects," *IEEE Transactions on Antennas and Propagation*, Vol. 54, No. 4, 1232–1242, 2006.
3. Semenov, S. Y., V. G. Posukh, A. E. Bulyshev, Y. E. Sizov, and P. N. Repin, "Microwave tomographic imaging of the heart in intact swine," *Journal of Electromagnetic Waves and Applications*, Vol. 20, No. 7, 873–890, 2006.
4. Rosenthal, A. and M. Horowitz, "Inverse scattering algorithm for reconstructing strongly reflecting fiber bragg gratings," *IEEE Journal of Quantum Electronics*, Vol. 39, No. 8, 1018–1026, 2003.
5. Chen, X. and K. Huang, "Microwave imaging of buried inhomogeneous objects using parallel genetic algorithm combined with FDTD method," *Progress In Electromagnetics Research*, PIER 53, 283–298, 2005.
6. Popovic, M. and A. Taflove, "Two-dimensional FDTD inversescattering scheme for determination of near-surface material properties at microwave frequencies," *IEEE Transactions on Antennas and Propagation*, Vol. 52, No. 2, 2366–2373, 2004.

7. Huang, C. H., Y. F. Chen, and C. C. Chiu, "Permittivity distribution reconstruction of dielectric objects by a cascaded method," *Journal of Electromagnetic Waves and Applications*, Vol. 21, No. 2, 145–159, 2007.
8. Colton, D. and L. Paivarinta, "The uniqueness of a solution to an inverse scattering problem for electromagnetic waves," *Arc. Ration. Mech. Anal.*, Vol. 119, 59–70, 1992.
9. Isakov, V., "Uniqueness and stability in multidimensional inverse problems," *Inverse Problems*, Vol. 9, 579–621, 1993.
10. Sheen, D. and D. Shepelsky, "Uniqueness in the simultaneous reconstruction of multiparameters of a transmission line," *Progress In Electromagnetics Research*, PIER 21, 153–172, 1999.
11. Tikhonov, A. N. and V. Arsenine, *Solutions of Ill-posed Problem*, Winston, New York, 1977.
12. Hansen, P. C., *Rank Deficient and Discrete Ill-posed Problems: Numerical Aspects of Linear Inversion*, SIAM, Philadelphia, 1998.
13. Abubakar, A. and P. M. Van Den Berg, "Total variation as a multiplicative constraint for solving inverse problems," *IEEE Transactions on Image Processing*, Vol. 10, No. 9, 1384–1392, 2001.
14. Abubakar, A., P. M. Van Den Berg, T. M. Habashy, and H. Braunisch, "A multiplicative regularization approach for deblurring problems," *IEEE Transactions on Image Processing*, Vol. 13, No. 11, 1524–1532, 2004.
15. Chung, Y. S., C. Cheon, and S. Y. Hahn, "Reconstruction of dielectric cylinders using FDTD and topology optimization technique," *IEEE Transactions on Magnetics*, Vol. 36, No. 4, 956–959, 2000.
16. Rekanos, I. T. and A. Raisanen, "Microwave imaging in the time domain of buried multiple scatterers by using an FDTD-based optimization technique," *IEEE Transactions on Magnetics*, Vol. 39, No. 3, 1381–1384, 2003.
17. Abubakar, A., T. M. Habashy, and P. M. Van Den Berg, "Nonlinear inversion of multi-frequency microwave fresnel data using the multiplicative regularized contrast source inversion," *Progress In Electromagnetics Research*, PIER 62, 193–201, 2006.
18. Taflove, A. and S. C. Hagness, *Computational Electrodynamics: The Finite-difference Time-domain Method*, 3rd edition, Artech House, 2005.
19. Semnani, A. and M. Kamyab, "An enhanced method for inverse scattering problems using Fourier series expansion in conjunction

with FDTD and PSO," *Progress In Electromagnetics Research*, PIER 76, 45–64, 2007.

20. Meyer, T., A. Jostingmeier, and A. S. Omar, "Microwave imaging using a novel regularization scheme," *Proceedings of the Antennas and Propagation Society International Symposium*, Vol. 3, 175–178, 2003.
21. Khalaj-Amirhosseini, M., "Reconstruction of inhomogeneous dielectrics at microwave frequencies," *Progress In Electromagnetics Research*, PIER 77, 75–84, 2007.
22. Robinson, J. and Y. Rahmat-Samii, "Particle swarm optimization in electromagnetics," *IEEE Transactions on Antennas and Propagation*, Vol. 52, No. 2, 397–407, 2004.
23. Lee, K. C. and J. Y. Jhang, "Application of particle swarm algorithm to the optimization of unequally spaced antenna arrays," *Journal of Electromagnetic Waves and Applications*, Vol. 20, No. 14, 2001–2012, 2006.
24. Chen, T. B., Y. L. Dong, Y. C. Jiao, and F. S. Zhang, "Synthesis of circular antenna array using crossed particle swarm optimization algorithm," *Journal of Electromagnetic Waves and Applications*, Vol. 20, No. 13, 1785–1795, 2006.